

# An Earthworm-Like Robotic Endoscope System for Human Intestine: Design, Analysis, and Experiment

KUNDONG WANG, GUOZHENG YAN, GUANYING MA, and DONGDONG YE

Department of Instrument Engineering, Shanghai Jiaotong University, No. 800 Dongchuan Road, Shanghai 200240, China

(Received 3 April 2007; accepted 31 October 2008; published online 12 November 2008)

**Abstract**—The existing endoscope brings too much discomfort to patients because its slim and rigid rod is difficult to pass through  $\alpha$ ,  $\gamma$  loop of the human intestine. A robotic endoscope, as a novel solution, is expected to replace the current endoscope in clinic. A microrobotic endoscope based on wireless power supply was developed in this paper. This robot is mainly composed of a locomotion mechanism, a wireless power supply subsystem, and a communication subsystem. The locomotion mechanism is composed of three liner-driving cells connected with each other through a two-freedom universal joint. The wireless power supply subsystem is composed of a resonance transmit coil to transmit an alternating magnetic field, and a secondary coil to receive the power. Wireless communication system could transmit the image to the monitor, or send the control commands to the robot. The whole robot was packaged in the waterproof bellows. Activating the three driving cells under some rhythm, the robot could creep forward or backward as a worm. A mathematic model is built to express the energy coupling efficiency. Some experiments are performed to test the efficiency and the capability of energy transferring. The results show the wireless energy supply has enough power capacity. The velocity and the navigation ability in a pig intestine were measured in *in vitro* experiments. The results demonstrated this robot can navigate the intestine easily. In general, the wireless power supply and the wireless communication remove the need of a connecting wire and improve the motion flexibility. Meanwhile, the presented locomotion mechanism and principle have a high reliability and a good adaptability to the *in vitro* intestine. This research has laid a good foundation for the real application of the robotic endoscope in the future.

**Keywords**—Wireless power supply, Wireless communication system, Locomotion mechanism, *In vitro* experiments.

## INTRODUCTION

It is reported about 90% of malignant tumors of the colon develop from some benign intestinal polyps.<sup>2</sup> In general, most of benign polyps do not have the

remarkable clinical symptom. The endoscope is an important procedure for gastrointestinal examination. As an invasive inspection, it is only used for some patients with certain symptom, so the cancer is always found in its late stage. If this polyp could be cut away in its early stage, the death rate led by the gastrointestinal malignant tumors would be reduced greatly. If the examination of full gastrointestinal is included in an ordinary health care, this question can be resolved well.

Since 1960, enteroscopes have been used extensively. This device with a slim rigid shaft is 2–2.5 m long. When a doctor exerts force to insert it into the patients' gastrointestinal, the patients often feel discomfort very much because the rigid rod of the endoscope squeezes the intestine wall. Additionally, the doctor needs a long time to be trained for the required skills, and the device only reaches 1/3 of the small intestine, leaving the rest unexamined. So the endoscope examination is far from a routine in health care.

At present, a swallowable capsule endoscope is applied to examine the full small intestine.<sup>5</sup> After ingestion, the capsule powered by a mini cell is advanced by the natural squirm of the intestine. In the mean time, the images are transmitted to the outer monitor wirelessly. At last, it is naturally excreted from the body, so the patients will not feel any discomfort during the examination. But it cannot inspect the full gastrointestinal because of the limited cell capacity. Additionally, the doctor cannot perform the repeating examinations to a lesion carefully because the capsule is not operated. So the capsule endoscope has a relatively high residual error ratio. Now, it is used only as an auxiliary diagnosis in clinic.

Recently, an autonomous robotic endoscope with a small size and a flexible body was used for inspecting the full gastrointestinal noninvasively. The robot, configured with some clinical instruments such as a biopsy forceps and a drug spray device, can be controlled to stop, or advance, or go backward by the doctor. Dario

Address correspondence to Kundong Wang, Department of Instrument Engineering, Shanghai Jiaotong University, No. 800 Dongchuan Road, Shanghai 200240, China. Electronic mail: kdwang@sjtu.edu.cn

developed an inchworm-like pneumatic robot with vacuum absorption to the colon wall.<sup>3</sup> The robot pulled an air tube for driving force. Wang proposed an earthworm-like robotic colonoscope actuated by three linear direct current (DC) motors with a wire cable.<sup>18</sup> However, the powered-actuated robot must haul an electric wire, and the pneumatic robot must load an air pipe too. This wire or pipe prevents the robot from entering the deep place of the intestine. The robot cannot examine the full small intestine, so the wire or the air pipe must be removed. Menciassi presented a capsule robotic endoscope with claws to fix itself on the intestine wall.<sup>12,13</sup> The robot uses a power supply on board. The predicted power consumption will reach 800 mW, a challenging value to the power source. Kim developed an earthworm-like robotic endoscope actuated by the shape memory alloy (SMA) actuators.<sup>8,9</sup> The power is supplied by a coin battery. The estimated working time is 8 min. Examining the intestine with 10-m length requires more power capability. Current cell is far away from the required one. Wireless energy supply based on electric magnetic coupling can provide the power continuously. This technology is used for the percutaneous energy transferring (PET), but this technology cannot be feasible in the robotic power supply.<sup>7,15-17</sup> First, its transferring distance is only several millimeters while the transferring distance needs more than 200 mm. Because the magnetic field is very sensitive to the distance variation, the received power is very limited. Second, the energy receiving part is fixed with regard to the energy transmitting part in the PET, while the position and the pose of robot as a supplied goal continue to vary randomly. The mismatch between the transmitting part and the receiving part leads to the very low energy transferring efficiency.

In this paper, a novel passive receiving coil (RC) is used to improve the power supply efficiency. The RC based on the principle of the gyroscope can hold a proper pose to match the transmitting coil (TC) well. Additionally, reducing the drivers' consumption is taken into account. The driver is composed of a micro-DC motor with high mechanical efficiency and small power consumption. Three motors, a power source circuit and a microcontroller are assembled together. By power supply with the wireless energy transferring method, an earthworm squirm is realized in a soft glue tube and *in vitro* pig colon. At last, some experiments and discussion about the locomotion efficiency are performed.

## SYSTEM OVERVIEW

The earthworm belongs to the Oligochaeta in the Annelida phylum, which comprises a deformable body

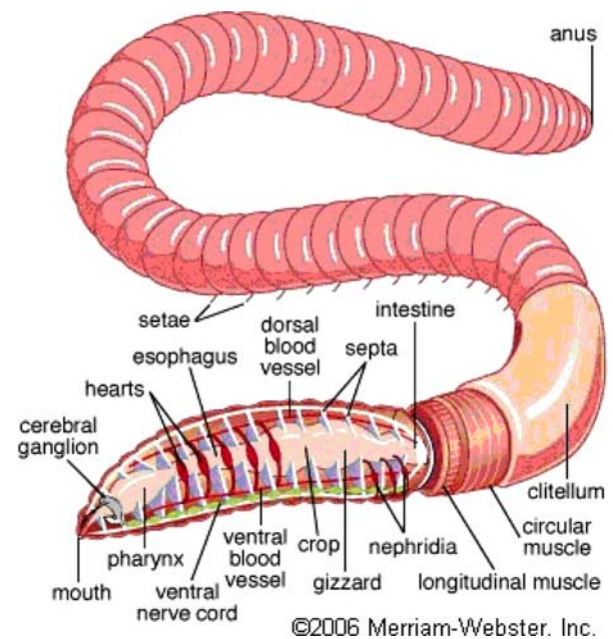


FIGURE 1. The dissection diagram of earthworm.

cavity, soft tissues, and incompressible coelomic fluid as shown in Fig. 1. A circular muscle and a longitudinal muscle form a mobile cell. Its locomotion principle is based on periodic traveling wave generated by its alternately triggering the mobile cell.<sup>1</sup> Friction difference among the mobile cells plays an important role in motion. According to the locomotion characteristics, the following principle should be considered carefully. First, the robot cannot tug a wire cable, so the communication and the power supply problem must be solved by wireless method. Second, the robot dimension must be designed as small as possible; finally, the robot must be controlled by the operator. It can stop, or go forward, or go backward to examine the suspected lesion. The microrobotic endoscope system is designed as shown in Fig. 2.

The system mainly comprises four modules including an earthworm like microrobot, an image module, an energy module, and a communication module as shown in Fig. 2. Energy or data exchange between the robot and the three modules is realized through the wireless technology.

A CMOS image sensor and an image data emitter are integrated into the image module, powered by an independent energy receiver. The emitter transfers the data to the receiver through antenna 1, MPU 1, that is the microprocessor unit 1, sends the data from the receiver to the computer through an I/O device. The image is displayed and processed in the special software. As a carrier of the image cell, the robot was actuated by the traction mechanism, which is composed of three locomotion cells. Each cell is connected with each other

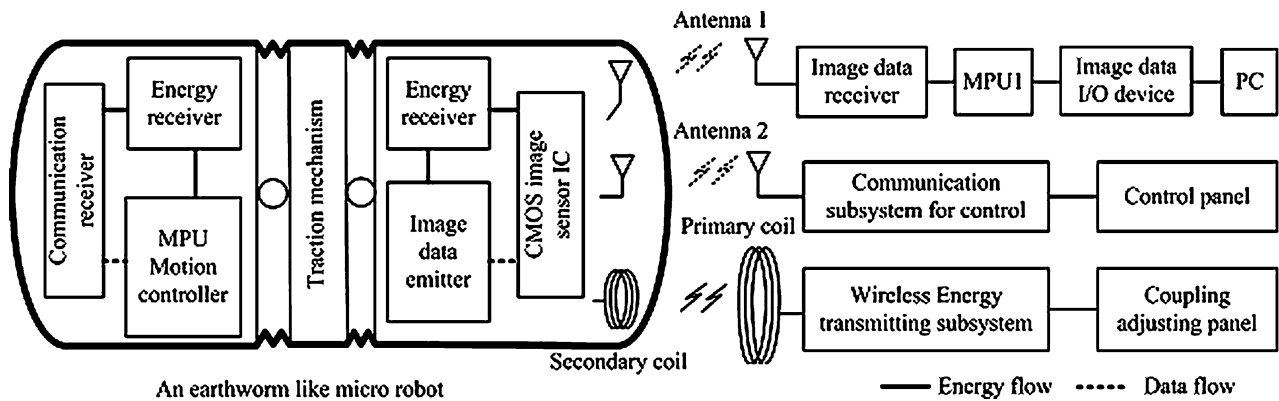


FIGURE 2. A microrobotic endoscope system.

by two-degree-of-freedom joints for good flexibility. MPU motion controller provides the traction mechanism with control signals. Communication receiver gets the command from the communication subsystem through the antenna 2, which can control the robot to go forward or backward, or to stay at a specified place interesting a doctor. Control panel is used to input the doctor's command. The locomotion cell is powered by another independent energy receiver. Both energy receivers get the energy from the coupling between the transmit coil and the secondary coil. Coupling adjustment panel is used to adjust the TC's voltage and current. Both the locomotion cell and the image cell are sealed by an emulsion film sleeve, which makes the outer surface of the robot like an earthworm's skin.

## DESIGN OF KEY MODULES

According to the above presentation, this wireless robotic endoscope is composed of three key modules including the robot module, the wireless energy module, and the wireless communication module. The microrobot is a launch vehicle for loading the camera, so the robot should be realized prior to other modules. Then for entering the deep place of the human gastrointestinal, the wireless energy transferring module is added into the robot system for cutting off the wire tail. Additionally, the wireless communication module transmits the image from the inner body to the outer body, and sends the operator's commands to the robot for active motion control. The following section will focused on the details of every module's realization.

### *The Earthworm-Like Microrobot Using DC Motor*

In the previous study, many researchers presented all kinds of locomotion methods including pneumatic driver, SMA driver, piezoelectric (PZT) driver.<sup>20</sup> In

fact, these drivers are not proper to be applied in the wireless robot for gastrointestinal. Pneumatic drivers cannot cast off its gas pipe. SMA driver's speed is very low because of its too long period of heating and cooling in enclosed intestinal environment.<sup>14</sup> PZT driver only produces displacement with micrometer order, while the required one is centimeter order. It is difficult to manufacture the mechanism for enlarging the displacement in a narrow space. In this paper, a magneto DC motor is selected as a driver because of its big energy transfer coefficient and low power consumption. There are three questions to be solved in the next. The first is to decrease the rotary speed and increase the torque output. The second is to transfer the rotary motion into the linear motion. The third is to control the motor's motion.

The speed reducer with total ratio 31.2 is shown in Fig. 3. The reducer with a four-stage reduction ratio includes 13 gears and 5 shafts. The gear is welded on the shaft by a laser spot welder. The shaft is supported on the jewel bearing embodied in the end cover. For smooth running, gear sets are installed symmetrically to eliminate the radial play of the gear set.

The motion transferring mechanism is shown in Fig. 4. A screw pair is used to transfer the rotation of the screw to the linear motion of the nut. Inner tube with a slot takes a role as a guide rod. Pin as a peg fixes the nut and the outer tube used to output the linear motion. When the screw rotates around, the nut will translate forward or backward because the slot of the inner tube constrains the revolution of nut. When the nut moves to the end of the inner tube, the probe will contact the electrode. The electrode connected with the high level is insulated with the mechanism by the insulation loop and insulation plate. When the probe connected with the low level contacts the electrode, the high level is pulled down to the low level. A port of the MPU detects the changing of probe's level, and the motor will be stopped when it goes to the end.

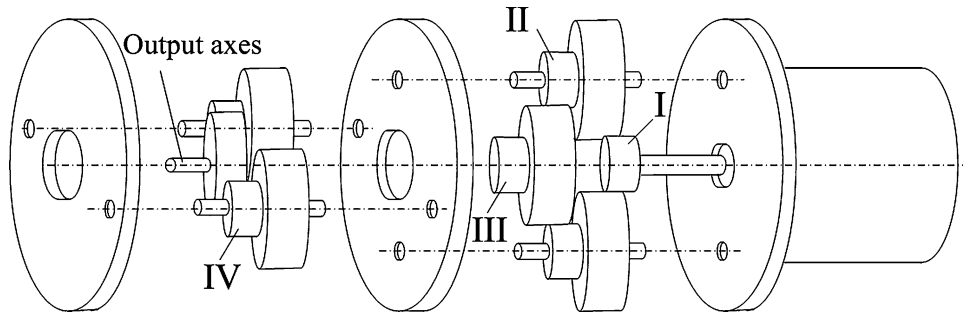
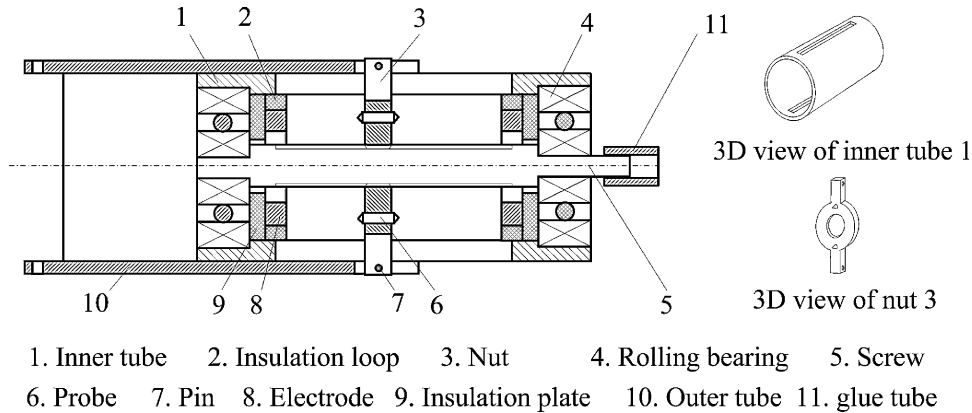


FIGURE 3. Explode view of the speed reducer.



1. Inner tube 2. Insulation loop 3. Nut 4. Rolling bearing 5. Screw  
6. Probe 7. Pin 8. Electrode 9. Insulation plate 10. Outer tube 11. glue tube

FIGURE 4. Motion transferring mechanism.

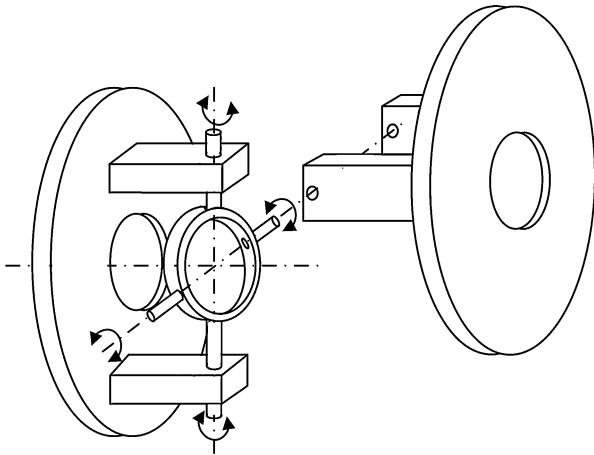


FIGURE 5. Passive joint with two degrees of freedom.

A flexible glue tube is used to link the screw of motion transferring mechanism and the output axes of the speed reducer. A passive joint with two degrees of freedom connects two covers of the reducer and the motion transferring mechanism as shown in Fig. 5, which makes the locomotion cell flexible. The robotic locomotion mechanism is composed of three above locomotion cells. Two locomotion cells are connected

with each other by several two-degree-freedom joints shown as Fig. 5, too. The locomotion mechanism is shown in Fig. 6a. A medical silicon gel film is coated outside of the robot for waterproof. A locomotion process is a recycle from Phase 1 to Phase 5 in Fig. 6a, and the corresponding control signals are shown as Fig. 6b. Here, it is presumed that the locomotion cell will extend when a positive voltage is applied. Otherwise, the locomotion cell will shorten.  $u_1$ ,  $u_2$ , and  $u_3$  represent the control signals Motor 1, Motor 2, and Motor 3, respectively. Then the locomotion process can be divided into six phases. All locomotion cells are contracted at phase 1. From  $t_0$  to  $t_1$ , Motor 1 is applied with the positive voltage, and the head cabin is pushed forward. From  $t_1$  to  $t_2$ , Motor 1 and Motor 2 are applied with negative voltage and the positive voltage, respectively, so the Motor 1 is pushed and pulled forward by head cabin and Motor 2, respectively. From  $t_2$  to  $t_3$ , similar motion occurs, and then Motor 2 goes forward. From  $t_3$  to  $t_4$ , Motor 3 is applied with a negative voltage to be pulled forward. At  $t_4$ , the robot has gone forward a step. Next, the aforementioned procedure is repeated, and then the robot can creep continuously. If the control signal is inverted, the robot will creep backward.

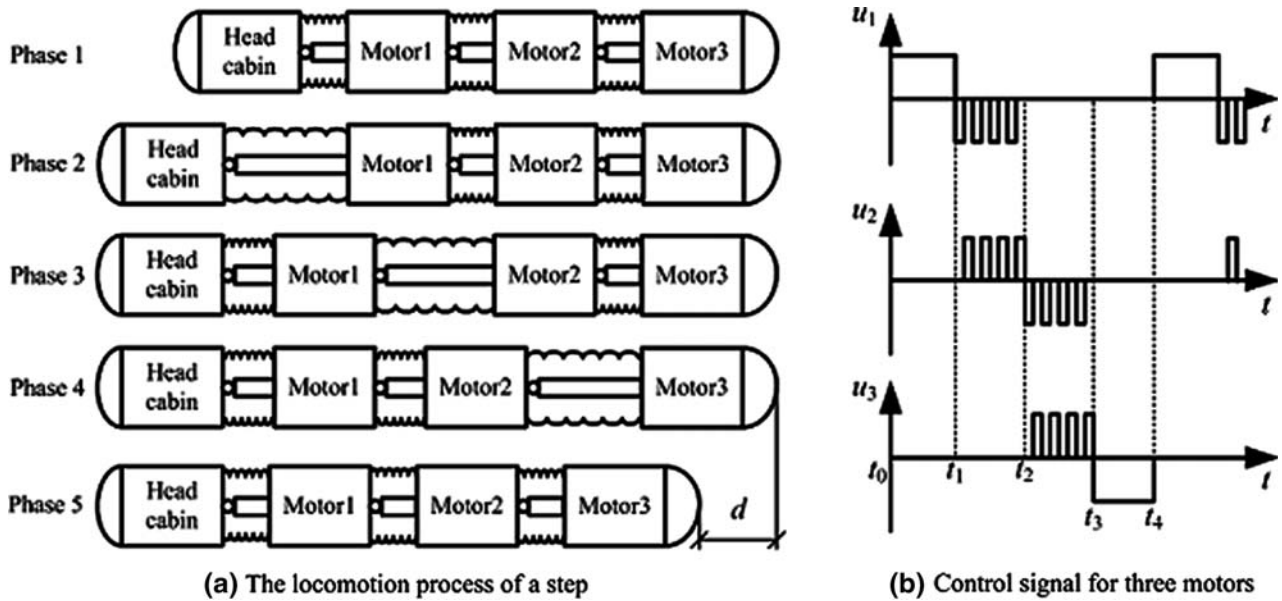


FIGURE 6. The motion control of the microrobot.

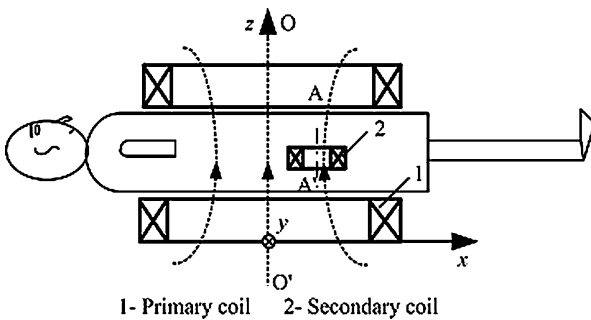


FIGURE 7. The geometrical relation between the TC and the RC.

*Wireless Energy Transmitting and Receiving Scheme*

Percutaneous energy transferring technology utilizes the magnetic field coupling of a TC and a RC to transfer the energy. In our study, the TC and the RC are installed as shown in Fig. 7. A patient lies on a test desk. Two TCs are placed above and under the body, respectively. An approximate parallel field is generated inside the human body, and the RC receives the energy for driving the robot.

It was reported this method can provide 36 Watt power for some implanted artificial organs, which was adequate to drive the robot. But this technology is not suitable here. In PET, the distance between the TC and the RC is not more than 20 mm, while the distance in robotic endoscope system exceeds 100 mm. The long distance leads to the fast attenuation of transmitting field, so the received power is very limited. Additionally, the RC of the implanted devices has the fixed

position and pose, while the RC in the robotic endoscope is moving together with the robot. So mismatch of the moving RC and TC in robotic endoscope system will lower the received power. In some bad case, the received power is near to zero.

For making up the attenuation, it's necessary to augment the transmitting power, specify the proper transmitting frequency to reduce the human absorption. In this system, a 10 kHz transmitting frequency is used. For holding, the RC not being mismatch with the TC, a float former like a gyro is used to support the TC. Its structure is shown in Fig. 8a and b. The float former is composed of an inner loop, a middle loop, an outer loop, a RC, and a bias weight. The middle loop is supported on the inner loop by a needle, which generates very little friction when the middle loop is rotating around axis Y. The outer loop has a similar structure with the middle loop. The middle loop can rotate around the axis X. Because the coil is fixed inside the inner loop, so the coil can rotate around not only axis X, but also axis Y. This structure can ensure that the centerline of the RC is always vertical in any case.

Its working principle is shown in Fig. 9. When the coil's centerline is deviated  $\alpha$  from vertical direction as shown in Fig. 9a, the bias weight will generate torque  $GD$  regarded to the axis X and the axis Y, where  $G$  is the gravity force of bias weight's barycenter and  $D$  is an arm of force. And then, the coil will return to the vertical direction at last as shown in Fig. 9b. For barrier-free rotation of the two loops, two leading wire ends of the coil are connected to the two metal needles of inner loop which are insulated with each other.

Two needles are tightly contacted with the metal middle loop in two machined pits, respectively. The machined pits are insulated with each other too. The needles on the middle loop play a similar role. At last, an induced electromotive force will generate on the two ports of the outer loop.

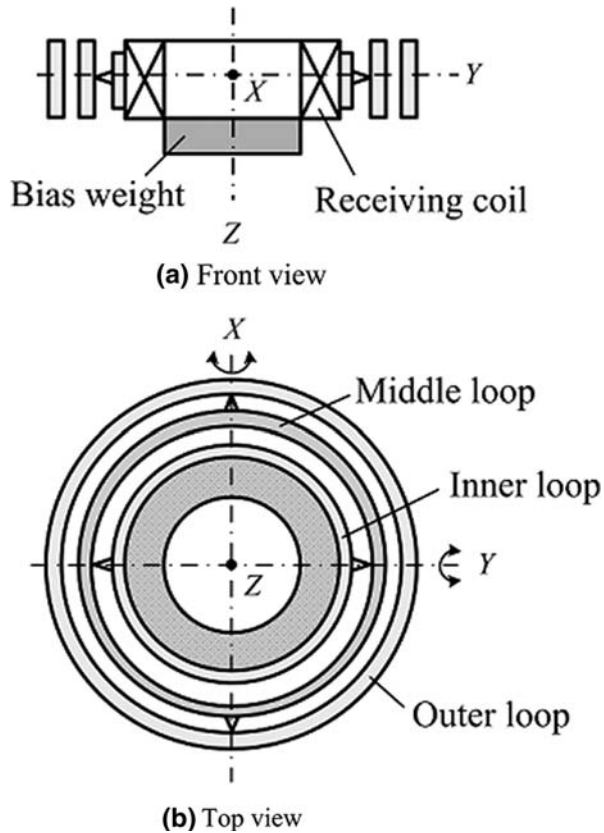
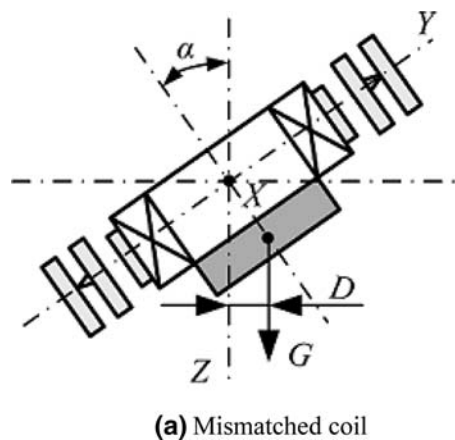
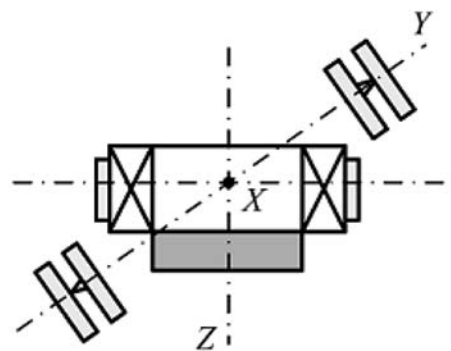


FIGURE 8. A gyro coil former for the receiving coil.



(a) Mismatched coil



(b) Pose of coil after adjustment

FIGURE 9. The receiving coil's adjustment.

### Wireless Remote Control Module

The wireless remote control module is composed of an outer controller and a motion controller as shown in Fig. 10. In the outer controller, if some button is pushed down, the corresponding port will be changed from high level to low level. MPU reads the port to judge which button is down, and then sends the defined command word wirelessly through the RF communication IC to the motion controller in the robot. In the motion controller, MPU reads the command word received by the RF communication IC. According to the command word, four ports of the MPU are programmed to generate the specified driving signals. In every locomotion cell, two position sensors are installed to determine whether the nut moves to the limiting position. When the nut of the locomotion cell reaches the end point, the corresponding key will be closed to pull down the level of MPU port. When the MPU detected the level change of the corresponding ports, it will turn on or off three analog switches S1, S2, and S3 to control the motor's on-off.

### PROTOTYPE ANALYSIS AND TESTING EXPERIMENTS

The micro robot prototype is shown in Fig. 11a. The robot is composed of five motion cells. The head cabin loads the camera. Next, three locomotion cells are connected in series. The end cabin carries the motion controller and TC. The compressible silicon gel bellow is installed between two cells for sealing. The robot shell is made of the anti-adhesive bio-compatible polymer material. These materials cannot be eroded by the strong acid liquid. The medical waterproof sealing gum filled up all gaps in the joint of the shell and the bellows.

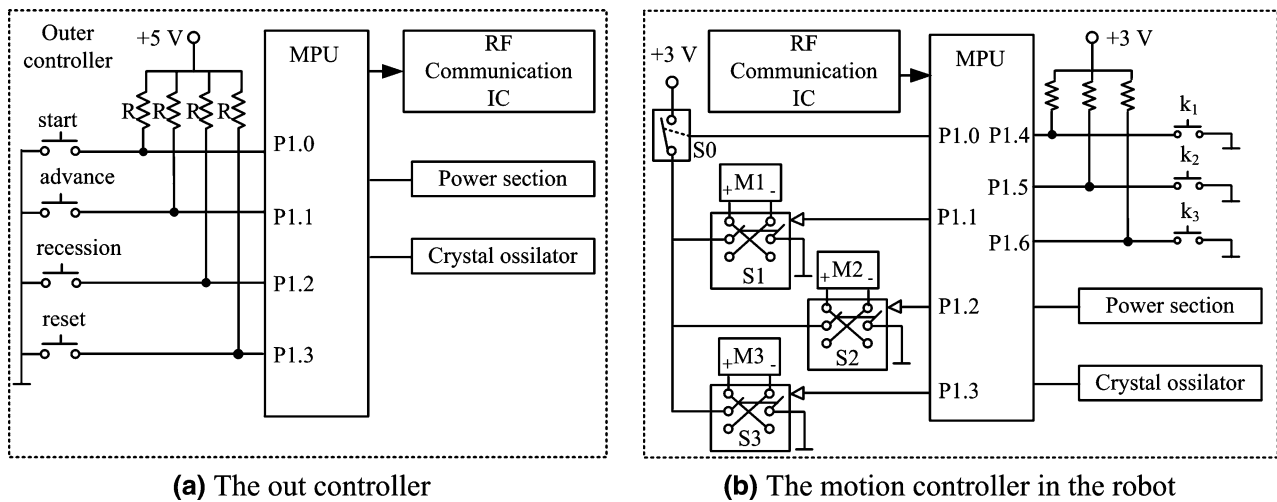
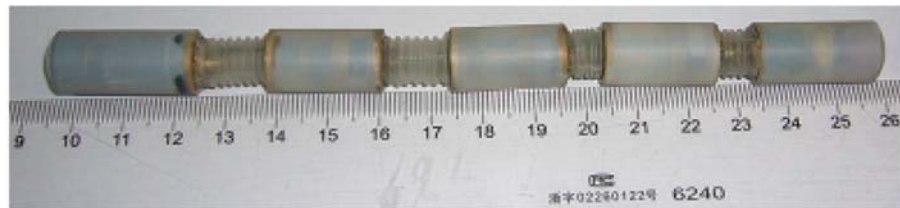


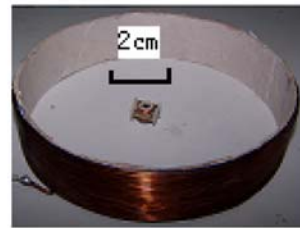
FIGURE 10. The control diagram for the microrobot.



(a) The prototype of robotic endoscope



(b) Linear driving cell



(c) Energy transferring coil



(d) Controller circuit

FIGURE 11. The micro earthworm-like robot prototype.

The camera uses a CMOS image sensor with model PO1200 from the Pixel Plus Corporation. The sensor containing an array of active pixel  $1600 \times 1200$  effective pixels can output NTSC/PAL composite video with 30 fps of frame rate. The current electric colonoscope in clinic often has a resolution of 0.8 megapixel. The 2.0 megapixel of the sensor can meet the requirement well. The camera uses a pinhole medical endoscopic lens with model EFL-1 of QINEIDA Inc. The imaging distance ranges from 1 to 100 mm.

Compared to the typical endoscopes with some holes to pass the biopsy forceps, water and air, the inside of the robotic endoscope is filled with the gears and the motors. In fact, the functions such as biopsy, spray, and hear therapy are also taken into account in

the robotic endoscope. In the head cabin, some space has been reserved to carry out the miniaturized diagnose or therapy medical components except the camera. The presented robotic endoscope is bent passively, which makes it unsuitable to examine the colon or the stomach with a larger cavity. But the wireless robotic endoscope can enter into the full small bowel noninvasively, which is difficult for the traditional endoscopes to examine. Additionally, because the small bowel is slim and smooth, the passive bended joints are adequate enough. We have developed a bent mechanism of head cabin in the previous research.<sup>19</sup> This mechanism has 10 mm diameter and 7 mm length. It has an independent controller and navigation algorithm based on vision. The mechanism can be installed

into the robot through replacing the passive joint between the head cabin and the traction mechanism. This research is now proceeding for lower power consumption and faster response. In future, this active bent articulation will be integrated into the robotic endoscope, which will extend the applications' range in clinic.

The robot's parameters are listed in Table 1. This size guarantees the robot to pass the narrowest part of the human intestine. The stroke  $S$  is the displacement when a motion cycle is repeated. The stroke must overcome the largest deformation of the intestine, which is determined by the mass, the diameter, the length of the locomotion cell, and the friction coefficient between the robot and the intestine inner wall.

The driving cell is comprised of a speed reducer with 31.2 reduction ratio, a screw pair to change the rotation into the linear motion, and a micro-DC motor as shown in Fig. 11b. The motor's cover has been installed on the DC motor, and the two-degree-freedom joint is used to link the reducer and the motion transfer mechanism, so it does not look like the designs shown in Figs. 3 and 4. The joint is mounted between the screw pair and the reducer, which makes the driving cell flexible. In the end of driving cell, another universal joint is used to link the later driving cell, so the robot's body is very flexible, which can adapt the uneven intestine. The TC and the RC are shown in Fig. 11c. Based on the gyroscopic principle, the RC's centerline is always parallel to the TC's centerline in any case, which guarantees the RC can receive enough energy. The coils' parameters are listed in the Table 2, which are determined by the restricted space in the robot, the power consumption of the robotic endoscope, and the available electrical parts such as the electric capacitor, the inductor.

In prototype analysis, two questions are considered. One is the energy transmitting efficiency; the other is the locomotion performances in different media. The following will be focused on the two questions.

**TABLE 1. The parameters of robotic design.**

Total length $L$ (mm)	Diameter $D$ (mm)	Stroke $S$ (mm)	Mass $m$ (g)
165	12	13	32

**TABLE 2. The required peak power of each module.**

Lighting LED	Camera	Communication	Locomotion cell	Controller
15 mW	65 mW	30 mW	290 mW	5 mW

### Test of the Energy Transmitting Efficiency

Total five modules are powered by the wireless energy supply. The required peak power of each module is listed in Table 2. The total power consumption reaches 405 mW. Although the five modules are not always working at the same time in the real locomotion, the maximum power consumption should be considered as the required minimum power for reliable motion.

In order to make sure that the robotic endoscope runs normally, the received power of RC must be larger than the required one. Additionally, electromagnetic safety is another key consideration essential to the medical endoscope. According to guide rule from International Commission on Non-Ionizing Radiation Protection (ICNIRP), Specific Absorption Rate (SAR) as a basic limited value cannot exceed 10 W/kg.<sup>6</sup> In term of the received power 500 mW, the localized SAR is about 0.4 W/kg, so the wireless energy transmitting method should be safe to the human body.<sup>11</sup> However, taking the endurable electromagnetic radiation limit of human body, the *in vitro* transmitting electromagnetic field should be reduced to the minimum under the condition that the received energy is sufficient. When a transmitting field is kept to be constant, the receiving efficiency determines the available power of RC. Here, a coupling coefficient is used to indicate the coupling degree between the RC and the TC shown as Fig. 7. It can be expressed as

$$k = \frac{M}{\sqrt{L_r \cdot L_t}}, \quad (1)$$

where  $k$  is the coupling coefficient,  $M$  is the mutual inductance of the two coil,  $L_r$  and  $L_t$  is the inductance of RC and TC, respectively.

The TC and the RC are regarded as a single coil, respectively. In the coordinate system  $xyz$  as shown in Fig. 12, the coordinate  $(x_1, y_1, z_1)$  of the point at the TC can be expressed as

$$\begin{cases} x_1 = R \cos \theta_1 \\ y_1 = R \sin \theta_1, \\ z_1 = 0 \end{cases} \quad (2)$$

where  $R$  is TC's radius, and  $\theta_1 \in [0, 2\pi]$ . The point  $(x_2, y_2, z_2)$  at the RC can be expressed as

$$\begin{cases} x_2 = r \cos \theta_2 \\ y_2 = r_0 + r \sin \theta_2 \\ z_2 = d_0 \end{cases} \quad (3)$$

where  $r$  is the radius of the RC, and  $\theta_2 \in [0, 2\pi]$ , and  $r_0$  is the distance between the axis  $AA'$  of RC and the axis  $OO'$  of TC, and  $d_0$  is the distance between the two single coils. If two elements are taken from the two



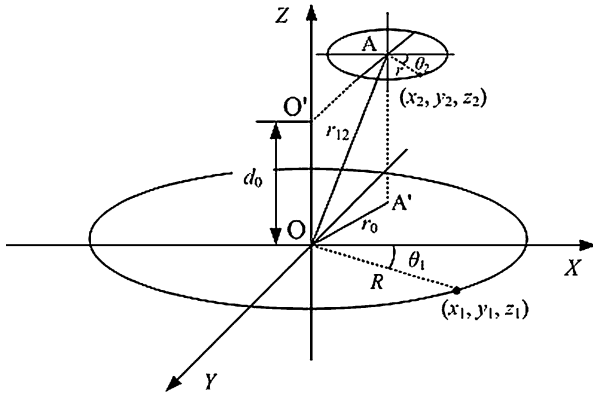


FIGURE 12. The space position of the two coils.

coil, respectively, the distance between the two elements can be written as:

$$r_{12} = \sqrt{(R\cos\theta_1 - r\cos\theta_2)^2 + (R\sin\theta_1 - r\sin\theta_2)^2 + d_0^2}. \quad (4)$$

According to Naumene equation, the mutual induction  $M_{12}$  between the two coils can be expressed as<sup>4</sup>:

$$M_{12} = \frac{\mu_0 R r}{4\pi} \int_0^{2\pi} \int_0^{2\pi} \frac{(\sin\theta_1 \cdot \sin\theta_2 + \cos\theta_1 \cdot \cos\theta_2)}{r_{12}} d\theta_1 d\theta_2. \quad (5)$$

The mutual induction  $M$  between a coil with  $N_1$  turns and the coil with  $N_2$  turns can be written as

$$M = N_1 N_2 M_{12}. \quad (6)$$

According to the reference, TC's self-inductance  $L_t$  can be written as<sup>10</sup>

$$L_t = 6.4\mu_0 N_1^2 R \cdot \frac{4R}{7R + 8l_t}, \quad (7)$$

where  $l_t$  is the coil's length, and  $\mu_0$  is the permeability of vacuum. Similarly, the RC's self-inductance  $L_r$  can be obtained too.

From Eqs. (1), (4–6), and (9),  $k$  can be written as

$$k = C \cdot \int_0^{2\pi} \int_0^{2\pi} \frac{(\sin\theta_1 \cdot \sin\theta_2 + \cos\theta_1 \cdot \cos\theta_2)}{r_{12}} d\theta_1 d\theta_2, \quad (8)$$

where  $C$  is defined as

$$C = \frac{1}{102.4\pi} \sqrt{(7R + 8l_t)(7r + 8l_r)}. \quad (9)$$

Equation (8) can be calculated through the numerical method. Through Eq. (8), the factors influencing  $k$

TABLE 3. The parameters of the two coils.

Coil type	Inner diameter (mm)	Width (mm)	Length (mm)	Turn
TC	270	40	20	82
RC	3.6	2.2	10	560

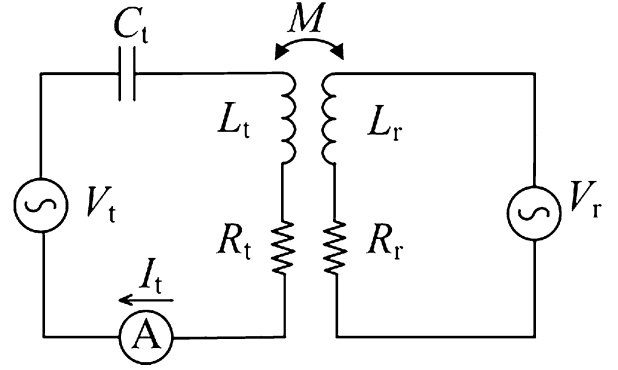


FIGURE 13. The circuit model of the energy transmitting subsystem.

can be explored in detail. In computation, the used parameters are listed in the Table 3.

In order to verify Eq. (8), a test circuit is designed as Fig. 13.  $L_t$ ,  $C_t$ , and  $R_t$  are the inductance, capacitance, and resistance of the TC, respectively.  $L_r$  and  $R_r$  are the inductance and resistance of the RC, respectively.  $V_t$  and  $I_t$  are voltage and current of the sine-wave input, respectively.  $V_r$  is the induced electromotive force.  $M$  is the mutual-inductance between two coils. Then according to the definition of the mutual induction,  $M$  can be written as

$$M = \frac{V_r}{2\pi f I_t}, \quad (10)$$

where  $f$  is the frequency of  $V_t$ . According to Eq. (1),  $k$  can be calculated through the following equation.

$$k = \frac{V_r}{2\pi f I_t \sqrt{L_r L_t}} \quad (11)$$

$L_t$  and  $L_r$  can be measured by an inductance meter. Obviously,  $k$  can be calculated through these measured values. In order to know about the changing law of coupling coefficient, the comparison between the experiment's result and Eq. (8) is performed as shown in Fig. 14. According to Fig. 14a,  $k$  decreases when the RC departs from the TC. When the RC deviated 40, 70, and 100 mm from the axis,  $k$ 's change tendency is the same. But when the deviation increases, the variation of  $k$  becomes smooth. Figure 14b indicates the

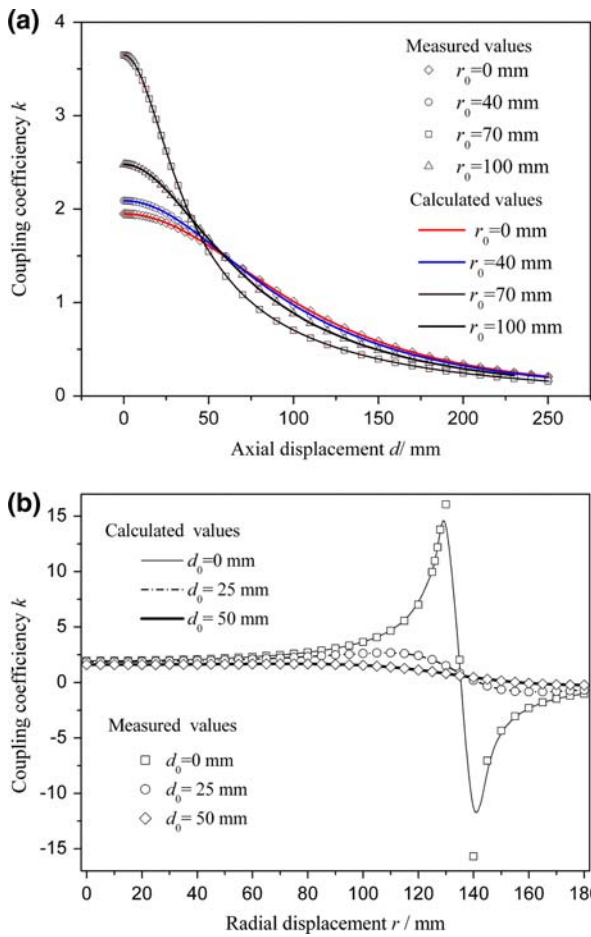


FIGURE 14. The changing law of the coupling coefficient  $k$ .

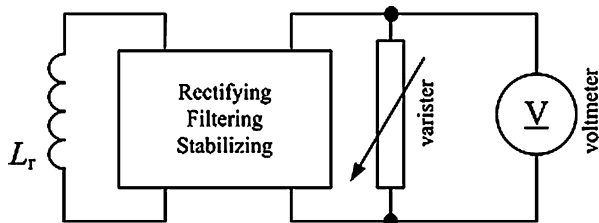


FIGURE 15. The test diagram of the maximum received power.

changing of coupling coefficient  $k$  along the radial displacement.

In the real application, the received power  $W$  must be larger than the power required by the robotic endoscope (Fig. 15). There are four modules consuming the power as shown in Table 2. The required total power is 405 mW. When the transmitting power is fixed,  $W$  varies with the changing of  $k$ . It's necessary to know about the distribution of  $W$  in space. A circuit is designed to test the maximum received power  $W_{max}$  as shown in Fig. 16. The RC generates the alternating

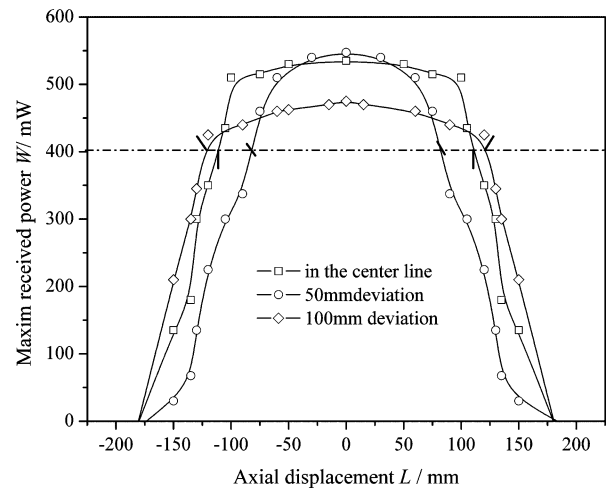


FIGURE 16. The distribution of the received power's maximum.

reduced electric force. After rectifying, filtering and stabilizing, the DC flows through the adjustable resistor. When the output voltage begins to fall down, the maximum received power  $W$  can be regarded as the product of the measured voltage output and current output.

When the deviation from the axis of TC is varied, the received power is shown in Fig. 16. When the RC moves along the axis of TC, the range of effective displacement is  $\pm 75$  mm, in which the received power is larger than 405 mW. When the deviations are 50 and 100 mm, the effective displacement ranges are  $\pm 130$  and  $\pm 150$  mm, respectively. This measurement shows that the energy transferring system is an effective method for power supply.

### Test of Locomotion Performance

The microrobot simulates the squirm of the earthworm living in the soft soil, which is expected to be safe and noninvasive to the soft intestine. But the intestine tissue, as a type of continuous viscous elastic solid material, is different from the unconsolidated soil greatly. Very little force will lead to the large deformation of the intestine. It was reported that the robotic stroke will be discounted by the intestine's displacement under the acting of the friction force between the robot and the intestine wall.<sup>18</sup> So it is necessary to verify this locomotion method's validity through some experiments *in vitro* intestine.

A fresh small bowel and a colon of pig are selected in the test. In order to approach the *vivi-intestine's* environment, the intestine is flushed only by saline. The mucous membrane is protected well from damage made by any other handling. The colon is laid on the desk as shown in Fig. 17a. The robot entered into the

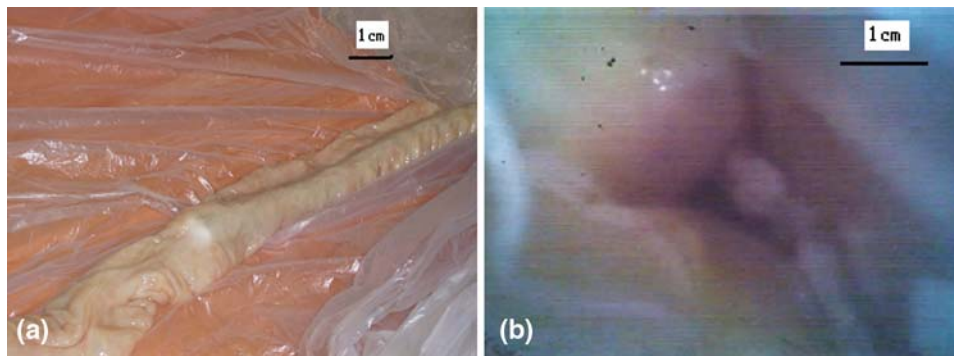


FIGURE 17. *In vitro* experiment of the robotic endoscope.

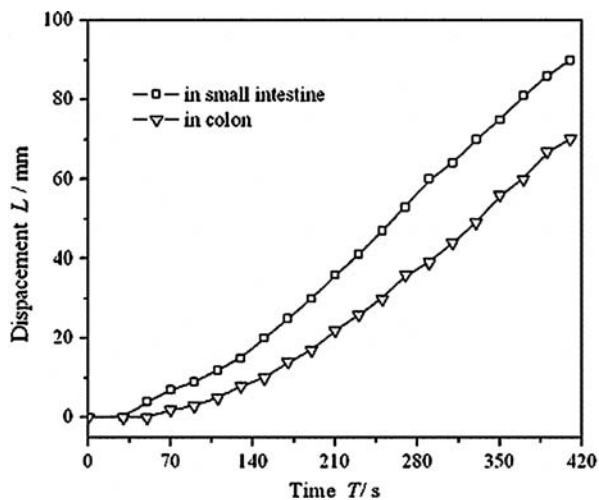


FIGURE 18. The measured velocity of the robotic endoscope.

intestine through an inserted glue tube. After turning the wireless energy system on, the robot began to move. In the mean time, the image is transmitted to the outer computer as shown in Fig. 17b. At the primal 2 min, the intestine was stretched tightly and the robot advanced a little distance about 5 mm. Then the robot moved on a larger speed than before. In some segment of the intestine, the robot advance back and forth well. For evaluating the motion performance of the robot, the relation between the displacement and the time is tested in the intestines as shown in Fig. 18. Obviously, the velocity in the small intestine is larger than the velocity in the colon. The inner surface of colon is uneven because of many microstructures, which lowers the motion efficiency. In contrast, the small intestine's wall is smoother than the colon's. So the higher efficiency can be found. This test indicates that the robot can advance in the intestine. But some disadvantages are found in the test. In the colon, the robot would be jammed once it entered into the dead area. For leaving this dead area, the robot had to perform the to-and-fro

movement. Jamming did not occur in the small bowel. Another important question is the robotic self-adaptability to the curving intestine. In the curvature, the robot spends more time than in the straight section.

## CONCLUSION

The robotic endoscope represents the developing tendency of the endoscope for human gastrointestinal. A novel wireless robotic endoscope is designed, analyzed, and tested in this paper. (1) The designed driving cell used a micromotor, a microreducer and a screw pair are featured with the low power consumption, the larger driving force and the big stroke; (2) the wireless power supply can provide enough energy for the robot; and (3) the robot has a satisfied motion performance in the *in vitro* experiment. This research has laid a foundation for the real application in clinic, but more works are needed to do in the future. The robot's mechanism can be optimized for smaller size and higher reliability. Enlarging the effective range of wireless power transferring system is another important issue for real application.

## ACKNOWLEDGMENT

The authors would like to make a grateful acknowledgement to the financial support from the High Technology Research and Development Program of China (2004AA404013 and 2008AA04Z201).

## REFERENCES

- Accoto, D., P. Castrataro, and P. Dario. Biomechanical analysis of Oligochaeta crawling. *J. Theoret. Biol.* 230:49–55, 2004. doi:10.1016/j.jtbi.2004.03.025.

- <sup>2</sup>Carrozza, M. C., L. Lenciomi, and B. Magnani. A micro robot for colonoscopy. In: Seventh International Symposium on Micro Machine and Human Science, Nagoya, Japan, 1996, pp. 223–228.
- <sup>3</sup>Dario, P., M. C. Carrozza, E. Guglielmelli, C. Laschi, A. Menciassi, and F. Vecchi. Robotics as a future and emerging technology: biomimetics, cybernetics, and neuro-robotics in European projects. *IEEE Robot. Automat. Mag.* 12:29–45, 2005.
- <sup>4</sup>Fang, D. Electrician Reckoner. Jinan, China: Shandong Science and Technology Press, 1994.
- <sup>5</sup>Iddan, G., A. Glukhovskiy, and P. Swain. Wireless capsule endoscopy. *Nature* 405(25):417, 2000. doi:[10.1038/35013140](https://doi.org/10.1038/35013140).
- <sup>6</sup>International Commission on Non-Ionizing Radiation Protection, Guidelines for limiting exposure to time-varying electric, magnetic, and electromagnetic fields (up to 300 GHz). Oxford, UK: Oxford University Press, 1998.
- <sup>7</sup>Joung, G. B., and B. H. Cho. An energy transmission system for an artificial heart using leakage inductance compensation of transcutaneous transformer. *IEEE Trans. Power Electr.* 13(6):1013–1022, 1998.
- <sup>8</sup>Kim, B., M.G. Lee, Y.P. Lee, Y.I. Kim, and G. Lee. An earthworm like micro robot using shape memory alloy actuator. *Sens. Actuat. A* 125:429–437, 2006. doi:[10.1016/j.sna.2005.05.004](https://doi.org/10.1016/j.sna.2005.05.004).
- <sup>9</sup>Kim, B., S.-H. Park, Y. J. Chang, *et al.* An earthworm-like locomotive mechanism for capsule endoscopes. In: IEEE International Conference on Robotics and Automation. Barcelona: IEEE, 2005, pp. 1205–1211.
- <sup>10</sup>Kraus, J. D., and D. A. Fleisch. Electromagnetics with Applications. Beijing, China: Tsinghua University Press, McGraw-Hill, 105 pp.
- <sup>11</sup>Ma, G. Research on a Miniature Robot and Wireless Powering Techniques for Intestine Inspection. Shanghai, China: Shanghai Jiaotong University, pp. 89–91, 2008.
- <sup>12</sup>Menciassi, A., and P. Dario. Bio-inspired solutions for locomotion in the gastrointestinal tract: background and perspectives. *Phil. Trans. R. Soc. Lond. A* 5:1–12, 2003.
- <sup>13</sup>Menciassi, A., S. Gorini, A. Moglia, *et al.* Clamping tools of a capsule for monitoring the gastro intestinal tract. In: IEEE International Conference on Robotics and Automation, Barcelona, Spain, 2005, pp. 1309–1314.
- <sup>14</sup>Menciassi, A., S. Gorini, G. Pernorio, and P. Dario. A SMA actuated artificial earthworm. In: IEEE International Conference on Robotics and Automation, New Orleans, LA, 2004, pp. 3282–3287.
- <sup>15</sup>Ozeki, T., T. Chinzei, and Y. Abe. A study on an energy supply method for a transcutaneous energy transmission system. *Artif. Organs.* 27(1):68–72, 2000.
- <sup>16</sup>Sato, F., T. Nomoto, and G. Kano. A new contactless power-signal transmission device for implanted functional electrical stimulation (FES). *IEEE Trans. Mag.* 40(4):2964–2966, 2004. doi:[10.1109/TMAG.2004.830416](https://doi.org/10.1109/TMAG.2004.830416).
- <sup>17</sup>Wang, G., W. Liu, and R. Bashirullah. A closed loop transcutaneous power transfer system for implantable devices with enhanced stability. In: ISCAS, 2004, pp. 17–20.
- <sup>18</sup>Wang, K., and G. Yan. Micro robot prototype for colonoscopy and in-vitro experiment. *J. Med. Eng. Technol.* 31(1):24–28, 2007. doi:[10.1080/03091900500233759](https://doi.org/10.1080/03091900500233759).
- <sup>19</sup>Wang, K., G. Yan, and J. Zuo. Active micro robot colonoscopy's navigation based on vision. *High Technol. Lett.* 16:372–376, 2006.
- <sup>20</sup>Yan, G.-Z., Q.-H. Lu, G. Q. Ding, *et al.* The prototype of a piezoelectric medical micro robot. In: International Symposium on Micromechatronics and Human Science. Nagoya: IEEE, 2002, pp. 73–78.